

## LETTERS

# Reflected light from sand grains in the terrestrial zone of a protoplanetary disk

William Herbst<sup>1</sup>, Catrina M. Hamilton<sup>2</sup>, Katherine LeDuc<sup>1</sup>, Joshua N. Winn<sup>3</sup>, Christopher M. Johns-Krull<sup>4</sup>, Reinhard Mundt<sup>5</sup> & Mansur Ibrahimov<sup>6</sup>

In the standard model of terrestrial planet formation, the first step in the process is for interstellar dust to coagulate within a protoplanetary disk surrounding a young star, forming large grains that settle towards the disk plane<sup>1</sup>. Interstellar grains of typical size  $\sim 0.1 \mu\text{m}$  are expected to grow to millimetre- (sand), centimetre- (pebble) or even metre-sized (boulder) objects rather quickly<sup>2</sup>. Unfortunately, such evolved disks are hard to observe because the ratio of surface area to volume of their constituents is small. We readily detect dust around young objects known as ‘classical’ T Tauri stars, but there is little or no evidence of it in the slightly more evolved ‘weak-line’ systems<sup>3</sup>. Here we report observations of a 3-Myr-old star, which show that grains have grown to about millimetre size or larger in the terrestrial zone (within  $\sim 3 \text{ AU}$ ) of this star. The fortuitous geometry of the KH 15D binary star system allows us to infer that, when both stars are occulted by the surrounding disk, it appears as a nearly edge-on ring illuminated by one of the central binary components. This work complements

the study of terrestrial zones of younger disks that have been recently resolved by interferometry<sup>4–6</sup>.

Figure 1 shows two views of the geometry of the KH 15D system according to our present interpretation. We adopt an updated version of model 3 of ref. 7 for all quantitative discussion. KH 15D is known to be a pre-main-sequence binary system with an age of  $\sim 3 \text{ Myr}$  and a distance of 760 pc (refs 8–10). It consists of  $0.6 M_{\odot}$  and  $0.7 M_{\odot}$  stars (designated A and B, respectively<sup>7</sup>;  $M_{\odot}$  is the solar mass) in an eccentric orbit ( $e = 0.6$ ) with a period of 48.37 days. Its orbit is inclined to a circumstellar disk that extends to  $\sim 5 \text{ AU}$  (ref. 11); precession of the disk is causing an occulting edge to advance across the orbit of the binary, as shown in Fig. 1b<sup>11,12</sup>. The precession timescale for the disk is  $\sim 1,000 \text{ yr}$ , and it must either be warped<sup>11</sup> or flared (or both) to cause both the foreground occultation and the background reflection. It is not known where, within this ring, the occulting edge is actually located—it could be at the inner or outer edge or at the high point of a warp somewhere in between. See Fig. 6 of the model paper<sup>7</sup> for a sketch of the possibilities.

For the past decade, only one star (A) has appeared above the disk edge, undergoing a dramatic ‘sunrise’ and ‘sunset’ every orbital cycle. During this time interval, the brightness of the system as measured at Earth has depended primarily on only one variable, namely the elevation ( $\Delta$ ) of star A above (or below) the ‘horizon’ defined by the edge of the occulting screen as projected on the plane of the sky. We

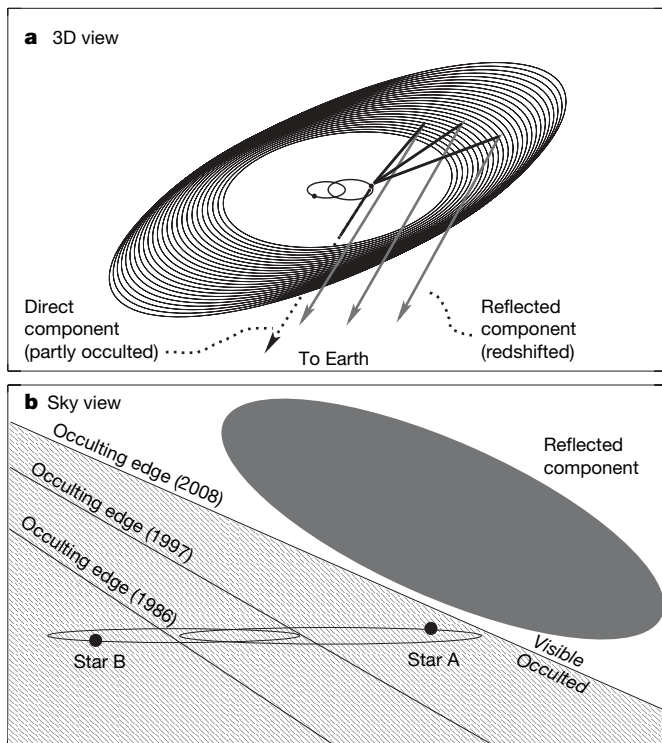
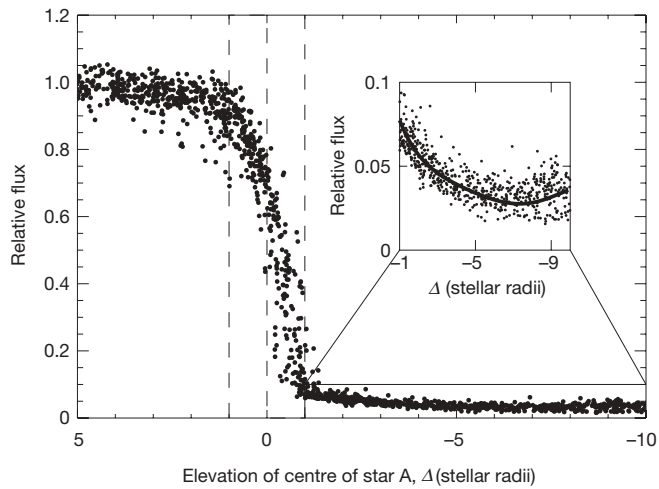


**Figure 1 | Schematic drawings showing our interpretation of the geometry of the KH 15D system.** **a, b,** Drawings showing a three-dimensional (3D) view (a) and a sky view (b). Only the part of the system to the right of the solid line in **b** is visible, owing to the opaque screen. The elliptical orbits of stars A and B are shown, as is the occulting edge, which advances from left to right. At present, the screen is just intercepting the outer edge of the orbit of star A, so that for a while, neither star will be seen above the occulting screen. The inner disk radius is located at 0.6 AU, which is approximately the location of the 3:1 orbital resonance that defines it according to dynamical models<sup>16</sup>. The outer disk is located at 5 AU, based on the precession timescale of  $\sim 1,000 \text{ yr}$  (refs 7, 11). The important difference between this model and others is that the reflected light is now recognized to come from evolved solids, probably of millimetre size, that have condensed in the terrestrial planet formation zone of this pre-planetary disk. Disks like this have long been hypothesized to exist as an intermediate step between the gas-rich, dust-laden disks seen around classical T Tauri stars and the so-called ‘debris’ disks seen around older stars such as  $\beta$  Pictoris<sup>17</sup> that contain dust due to fragmenting collisions between metre- or kilometre-sized planetesimals. The KH 15D disk is remarkably dust-free, and represents an intermediate stage between a classical T Tauri star disk and a debris disk. Although not depicted here, there is still some gas in the disk, as evidenced by weak accretion signatures, including forbidden lines of sulphur and oxygen and extended emission wings to hydrogen lines<sup>18,19</sup>.

<sup>1</sup>Astronomy Department, Wesleyan University, Middletown, Connecticut 06459, USA. <sup>2</sup>Physics and Astronomy Department, Dickinson College, Carlisle, Pennsylvania 17013, USA. <sup>3</sup>Department of Physics, Massachusetts Institute of Technology, 77 Massachusetts Avenue, Cambridge, Massachusetts 02139, USA. <sup>4</sup>Department of Physics and Astronomy, Rice University, Houston, Texas 77005, USA. <sup>5</sup>Max-Planck-Institut für Astronomie, Königstuhl 17, D-69117 Heidelberg, Germany. <sup>6</sup>Ulugh Beg Astronomical Institute of the Uzbek Academy of Sciences, Astronomicheskaya 33, 700052 Tashkent, Uzbekistan.



measure  $\Delta$  in units of the radius of star A ( $1.3R_{\odot} \approx 10^9$  m;  $R_{\odot}$  is the solar radius). Figure 2 shows the system brightness at  $0.80 \mu\text{m}$  wavelength, as a function of  $\Delta$ , during the last four years (ref. 13; K.L. *et al.*, manuscript in preparation). For  $\Delta > 1$ , the full disk of star A is

**Figure 2 | Brightness variation of KH 15D with elevation of star A.** Abscissa units are radii of star A ( $1.3R_{\odot} \approx 10^9$  m). Dashed lines show the points where the screen first contacts the limb of the star ( $\Delta = 1$ ), where the star is half obscured ( $\Delta = 0$ ) and where it is just fully obscured ( $\Delta = -1$ ). Inset, behaviour after occultation on a modified scale for clarity. The rise in brightness that occurs for elevations below  $-6$  is due to the influence of star B, which is closer to the screen edge than star A at those orbital phases. The solid line is a ‘proof-of-concept’ model of the light curve discussed in more detail in Supplementary Information. It represents a fifth-order polynomial fit to the predicted flux of the system based on the expression:

$$\text{Flux}(\Delta) = \exp[-\tau(A)] + 1.37\exp[-\tau(B)] + C_1 f_{\text{refl}}(\Delta) + C_2$$

where  $f_{\text{refl}}(\Delta) = \Omega_{\text{ring}}(A) + 1.37\Omega_{\text{ring}}(B)$ , and  $\Omega_{\text{ring}}$  is the solid angle subtended by the top of the disk (as a fraction of  $4\pi$  sr) as seen from the relevant star. The luminosity of star B is 1.37 times that of star A<sup>7,20,21</sup>. The disk is modelled as a flat ring of inner radius 0.5 AU and outer radius 5 AU (refs 11, 16). The exponential factors account for transmitted light, where  $\tau = 1.46 - 1.46\Delta$ . The parameters  $C_1$  and  $C_2$  were chosen to roughly fit the data by eye and have the values  $C_1 = 2.0$  and  $C_2 = 0.02$  for this ‘proof-of-concept’ model. Physically,  $C_1$  controls the relative amount of phase-dependent scattered light and depends on the geometry, albedo and phase function of the particles.  $C_2$  allows for a small amount of invariable scattered light. The maximum solid angle subtended by the top of the disk in our model is 0.43 sr for star A and 0.10 sr for star B.

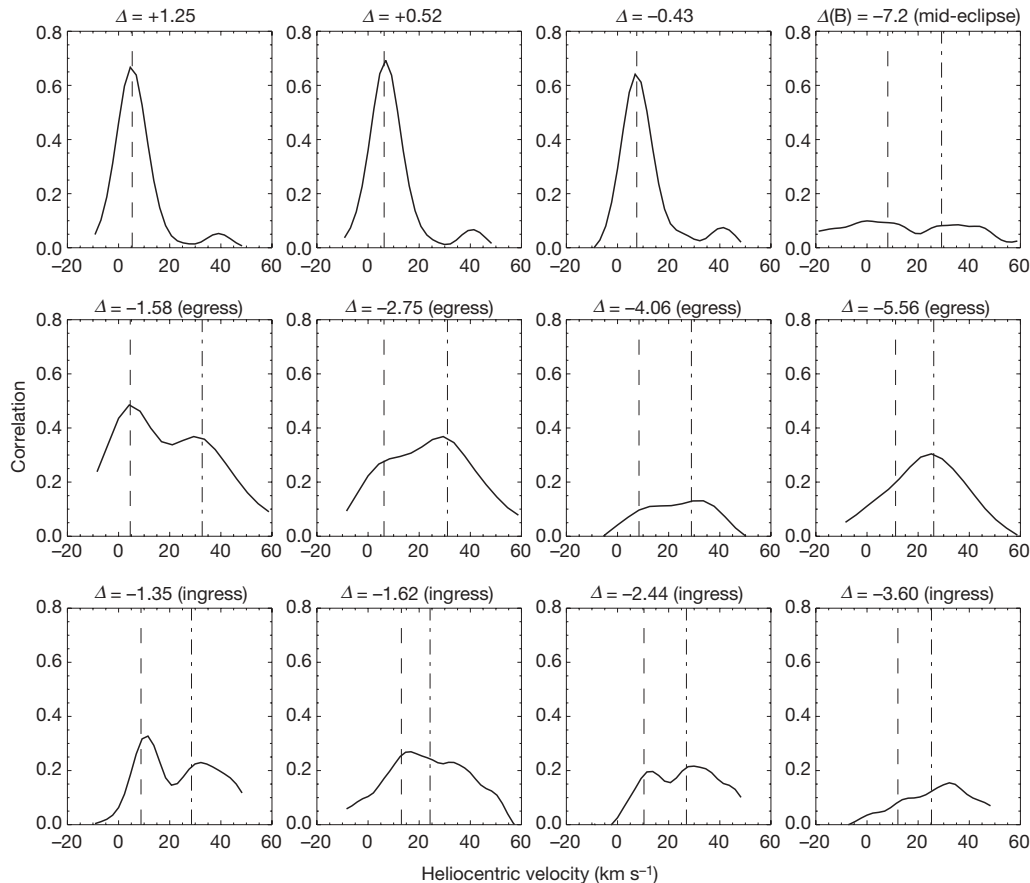


**Figure 3 | Spectral variation of KH 15D with elevation of star A.** Shown are cross-correlation functions of KH 15D spectra with a K7 V synthetic spectrum over the spectral range  $0.644\text{--}0.645 \mu\text{m}$ . The telescopes and instruments used were the 10 m Keck I telescope and HIRES echelle spectrometer, the UV–visual echelle spectrograph on the European Southern Observatory’s 8.2 m Very Large Telescope, and the 6.5 m Magellan II telescope and the MIKE echelle spectrometer. The spectral region includes several photospheric lines, primarily due to Ba I, and is not affected by emission lines or terrestrial features. The vertical dashed lines indicate the radial velocity of star A (or B, for the mid-eclipse spectrum) based on our model<sup>7,22</sup>. The dashed-dotted lines show the expected velocity of the reflected component if the mirroring particles had the systemic velocity of

$18.65 \text{ km s}^{-1}$  and were located directly behind the star from our vantage point. When  $\Delta > -1$ , the light from KH 15D is dominated by star A (upper row, left three panels). When star A is fully occulted from our vantage point (middle and bottom rows), but still visible to the reflecting particles on the top side of the back of the disk ( $-6 < \Delta < -1$ ), it is the reflected light from star A that contributes to the system’s light and produces the red-shifted radial velocity component. The spectrum in the upper-right panel was obtained near mid-eclipse in 2004, at a time when  $\Delta \equiv \Delta(A) = -7.6$  and  $\Delta(B) = -7.2$ . Hence, star B, which is also brighter, would be the expected source of most of the system’s light in our model, and its velocity and predicted reflection component are shown.

visible and the system's flux is determined by its brightness; for  $+1 > \Delta > -1$ , the star is partly occulted; and for  $\Delta < -1$ , it is fully occulted. As Fig. 2 inset shows, while the total light from the KH 15D system plummets precipitously in the interval  $+1 > \Delta > -1$ , it also continues to depend on  $\Delta$  even after full occultation ( $\Delta < -1$ ).

In earlier studies, the system's visibility after full occultation has been attributed to haloes of scattered light around each component or around the system as a whole<sup>7,14</sup>. Analysis of high-resolution spectra of the system when faint now paints a different picture. Figure 3 displays the cross-correlation functions of a number of high-resolution spectra with a K7 V synthetic spectrum. The spectra show a single strong peak at the radial velocity of star A for  $\Delta > -1$ , but become double-peaked after full occultation, with one peak corresponding to star A and the other to a red-shifted component. The radial velocity of the second component does not match star B, which is also far below the horizon at these times (see Fig. 1) and heavily obscured. We propose that the second peak is reflected light from the part of KH 15D's disk that is behind the stars from our vantage point. Star A is moving towards the Earth (relative to the systemic velocity of  $+18.65 \text{ km s}^{-1}$ ) during both ingress and egress, so its reflection from a mirror behind the star would appear to be moving away from us (red-shifted). During mid-eclipse, it is star B that is more elevated with respect to the obscuring edge and we may see its direct light (very dimly) and its reflection, as the upper-right panel in Fig. 3 shows. We find good agreement, especially during ingress, between the predicted radial velocities according to this interpretation and the observed velocities of the red-shifted components.

Our reflection model also accounts well for the shape of the light variations during full occultation, as we now discuss (see Supplementary Information for additional details). The inclination of the orbit to the ring means that, viewed from a point on the 'top surface' (that is, the surface visible from Earth) of the back side of the ring, only one star is fully visible at any time and its height above the local horizon

depends on the orbital phase. We assume that the brightness of the system is proportional to the solid angle subtended by the top of the ring as seen from the illuminating star. We also allow for a transmission component to the light, as required by the spectra. From simultaneous photometry obtained on three nights when we could separate the direct and reflected light, we can estimate the optical depth ( $\tau$ ) of the occulting screen as a function of  $\Delta$ . These data show that  $\tau = 2.9$  at  $\Delta = -1$  and that it increases roughly linearly with  $\Delta$ , as one would expect. The reflection is assumed to come from a flat ring with inner and outer radii of 0.5 AU and 5 AU, respectively; a representative model light curve is shown as the solid line in Fig. 2 inset. It reproduces the shape of the observed light curve quite well, in particular the brightening that occurs for  $\Delta < -6$  owing to the fact that star B has risen to become the illuminating star.

The data and our interpretation also permit us to derive constraints on the size of the grains that constitute the obscuring/reflecting disk. Figure 4 shows how the colour of the system changes during full occultation in the optical and near-infrared (Fig. 4a and b, respectively). Importantly, there is no evidence for reddening, which implies that the ring particles are significantly larger (by at least a factor of 20) than those in the interstellar medium<sup>14</sup>. Immediately after star A 'sets' ( $\Delta < -1$ ), some light from that star is still visible through the occulting part of the disk, allowing a measurement of the optical depth along that path length, which provides a further size constraint on the grains. In our model, the screen optical depth ( $\tau$ ) can be expressed as  $\tau = 64MR^{-2}r^{-1}\rho^{-1}(L/T)$ , where  $M$  is the total mass of obscuring particles (in Earth masses),  $R$  is the disk radius (in AU),  $r$  is the grain radius (in mm),  $\rho$  is the density of a grain (in  $\text{g cm}^{-3}$ ),  $L$  is the path length of the radiation through the obscuring medium, and  $T$  is the disk thickness. Our data show that  $\tau = 2.9$  at  $\Delta = -1$ , so for representative choices of  $\rho = 3$  and  $L/T = 0.05$ , we obtain  $r \approx \Sigma$ , where  $\Sigma$  is the mass surface density of the disk in Earth masses per square AU. Using our own Solar System as a guide, we may

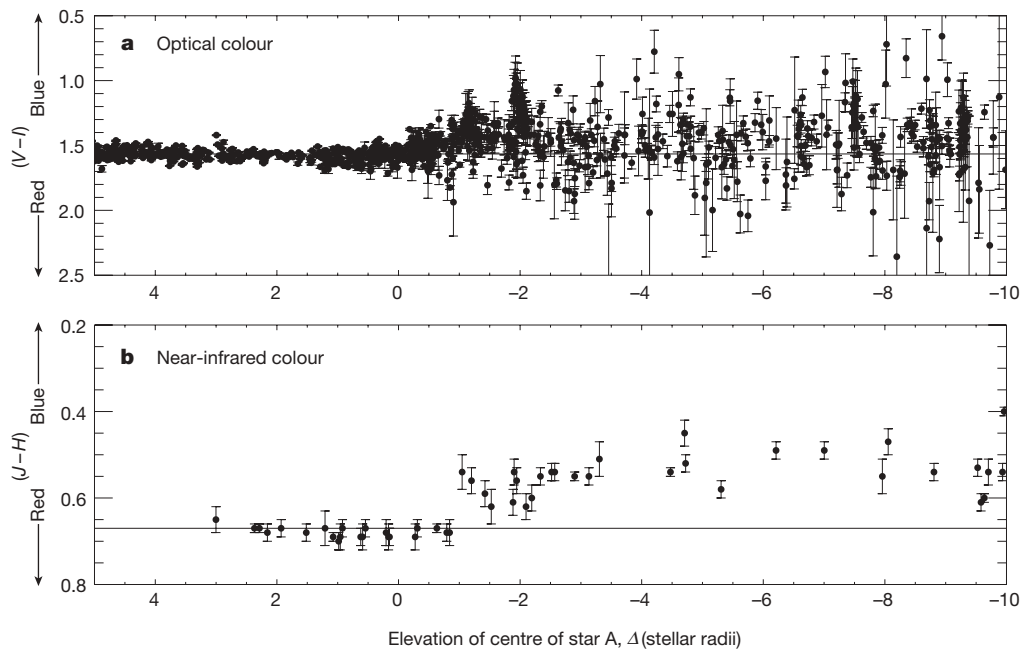


**Figure 4 | Colour variation of KH 15D with elevation of star A.** **a**, The  $V - I$  colour of the Cousins system (ref. 13; K.L. *et al.*, manuscript in preparation), with effective wavelengths at  $0.55 \mu\text{m}$  and  $0.80 \mu\text{m}$ , respectively; **b**, comparison of brightness in  $J$  ( $1.26 \mu\text{m}$ ) and  $H$  ( $1.66 \mu\text{m}$ )<sup>23</sup>. Error bars,  $\pm 1$  s.d. In the optical range, KH 15D has a stable colour before the beginning of the eclipse ( $\Delta > 1$ ), becomes steadily bluer during eclipse ( $1 > \Delta > -1$ ) and maintains the bluer colour during the phases when reflected light dominates ( $\Delta < -1$ ). In the near-infrared, there is also a transition to a bluer light during the reflection phases. The solid line shows the average colours out of eclipse. The blueness is consistent with what one might expect from

unweathered silicates having particle sizes significantly larger than in the interstellar medium<sup>24</sup>. Relatively blue spectral response is characteristic of some asteroidal material found in the Solar System, such as eucrites (pyroxene plus plagioclase feldspar). We further note that the shape of the albedo function is not consistent with scattering from grains of interstellar-medium size nor is the fact that most of the scattered light clearly arrives by back-scattering, not forward scattering. Finally, note that there is no evidence of reddening of the direct light of either star at any phase; the occulting screen shows no evidence of submicrometre-sized dust.

infer a grain size for this path length through the disk of roughly 1 mm. Interestingly, this is characteristic of chondrules, the glassy spherules that are a primary component of the most primitive meteorites found in our own Solar System<sup>15</sup>.

The most uncertain parameter in our expression for  $\tau$  is ( $L/T$ ), and this could be larger than the value of 0.05 we adopt, which would increase the inferred size of the grains. Our derivation (see Supplementary Information) assumes that the grains are uniformly distributed through a cylindrical volume of thickness  $T$ , where  $T$  is determined from the projected extent of the obscuring material on the plane of the sky. A more realistic picture may be that the grains are concentrated into a thinner structure, which is tilted, warped, corrugated and/or flared in such a way that its footprint of obscuration on the sky is much larger than its physical thickness. In this case  $L/T > 0.05$ , and one might have a disk composed of pebbles. Furthermore, if there were a vertical gradient of grain size within the disk, we would expect to be measuring the smallest grains present, as they would have the largest scale height. For both of these reasons, we consider our estimate of  $\sim 1$  mm to be characteristic of the smallest grains that could be present in the disk; the bulk of the disk might consist of even larger grains.

Received 11 September 2007; accepted 2 January 2008.

- Dominik, C., Blum, J., Cuzzi, J. N. & Wurm, G. in *Protostars and Planets V* (eds Reipurth, B., Jewitt, D. & Keil, K.) 783–800 (Univ. Arizona Press, Tucson, 2007).
- Natta, A. *et al.* in *Protostars and Planets V* (eds Reipurth, B., Jewitt, D. & Keil, K.) 767–781 (Univ. Arizona Press, Tucson, 2007).
- Wolk, S. J. & Walter, F. M. A search for protoplanetary disks around naked T Tauri stars. *Astron. J.* **111**, 2066–2076 (1996).
- van Boekel, R. *et al.* The building blocks of planets within the 'terrestrial' region of protoplanetary disks. *Nature* **432**, 479–482 (2004).
- Isella, A., Testi, L. & Natta, A. Large dust grains in the inner region of circumstellar disks. *Astron. Astrophys.* **451**, 951–959 (2006).
- Eisner, J. Water vapour and hydrogen in the terrestrial-planet-forming region of a protoplanetary disk. *Nature* **447**, 562–564 (2007).
- Winn, J. N. *et al.* The orbit and occultations of KH 15D. *Astrophys. J.* **644**, 510–524 (2006).
- Kearns, K. E. & Herbst, W. Additional periodic variables in NGC 2264. *Astron. J.* **116**, 261–265 (1997).
- Hamilton, C. M., Herbst, W., Shih, C. & Ferro, A. J. Eclipses by a circumstellar dust feature in the pre-main sequence star KH 15D. *Astrophys. J.* **554**, L201–L204 (2001).
- Herbst, W. *et al.* Fine structure in the circumstellar environment of a young, solar-like star: The unique eclipses of KH 15D. *Publ. Astron. Soc. Pacif.* **114**, 1167–1172 (2002).
- Chiang, E. I. & Murray-Clay, R. A. The circumbinary ring of KH 15D. *Astrophys. J.* **607**, 913–920 (2004).
- Winn, J. N., Holman, M. J., Johnson, J. A., Stanek, K. Z. & Garnavich, P. M. KH 15D: Gradual occultation of a pre-main sequence binary. *Astrophys. J.* **603**, L45–L48 (2004).
- Hamilton, C. M. *et al.* The disappearing act of KH 15D: Photometric results from 1995 to 2004. *Astron. J.* **130**, 1896–1915 (2005).
- Agol, E., Barth, A. J., Wolf, S. & Charbonneau, D. Spectropolarimetry and modeling of the eclipsing T Tauri star KH 15D. *Astrophys. J.* **600**, 781–788 (2004).
- Boss, A. P. in *Chondrules and the Protoplanetary Disk* (eds Hewins, R. H., Jones, R. H. & Scott, E. R. D.) 257–263 (Cambridge Univ. Press, New York, 1996).
- Artymowicz, P. & Lubow, S. H. Dynamics of binary-disk interaction. 1: Resonances and disk gap sizes. *Astrophys. J.* **421**, 651–667 (1994).
- Golimowski, D. A. *et al.* HST/ACS multiband coronagraphic imaging of the debris disk around Beta Pictoris. *Astron. J.* **131**, 3109–3130 (2006).
- Hamilton, C. M., Herbst, W., Mundt, R., Bailer-Jones, C. A. L. & Johns-Krull, C. M. Natural coronagraphic observations of the eclipsing T Tauri system KH 15D: Evidence of accretion and bipolar outflow in a weak-line T Tauri star. *Astrophys. J.* **591**, L45–L48 (2004).
- Tokunaga, A. T. *et al.* H<sub>2</sub> emission nebulosity associated with KH 15D. *Astrophys. J.* **601**, L91–L94 (2004).
- Johnson, J. A. & Winn, J. N. The history of the mysterious eclipses of KH 15D: Asiago Observatory, 1967–1982. *Astron. J.* **127**, 2344–2351 (2004).
- Johnson, J. A. *et al.* The history of the mysterious eclipses of KH 15D. II. Asiago, Kiso, Kitt Peak, Mount Wilson, Palomar, Tautenburg, and Rozhen Observatories, 1954–1997. *Astron. J.* **129**, 1978–1984 (2005).
- Johnson, J. A., Marcy, G. W., Hamilton, C. M., Herbst, W. & Johns-Krull, C. M. KH 15D: A spectroscopic binary. *Astron. J.* **128**, 1265–1272 (2004).
- Kusakabe, N. *et al.* Near-infrared photometric monitoring of the pre-main sequence object KH 15D. *Astrophys. J.* **632**, L139–L142 (2005).
- Burbine, T. H. & Binzel, R. P. in *Asteroids, Comets, Meteors 1993* (eds Milani, A., Di Martino, M. & Cellino, A.) 255–270 (Proc. IAU Symp. 160, Kluwer, Dordrecht, 1994).

**Supplementary Information** is linked to the online version of the paper at [www.nature.com/nature](http://www.nature.com/nature).

**Acknowledgements** This material is based on work supported by the US National Aeronautics and Space Administration (NASA) through the Origins of Solar Systems programme. Some of the data presented here were obtained at the W. M. Keck Observatory from telescope time allocated to NASA through the agency's scientific partnership with the California Institute of Technology and the University of California. The Observatory was made possible by the financial support of the W. M. Keck Foundation. We appreciate comments from E. Chiang, M. Gilmore, J. Greenwood and E. Jensen.

**Author Information** Reprints and permissions information is available at [www.nature.com/reprints](http://www.nature.com/reprints). Correspondence and requests for materials should be addressed to W.H. ([wherbst@wesleyan.edu](mailto:wherbst@wesleyan.edu)).